Systematic Polynomial-Based Modulation for Reduced Power Losses in DAB Converters

Alba Rodriguez-Lorente
M.A.C.I.M.T.E
Univ. Rey Juan Carlos
Mostoles, Spain
alba.rodriguez@urjc.es

Abraham M. Alcaide
Electronic Engineering Dept.
Univ. de Sevilla
Sevilla, Spain
amarquez@ieee.org

Jose I. Leon
Electronic Engineering Dept.
Univ. de Sevilla
Sevilla, Spain
jileon@us.es

Andres Barrado
Electronics Department
Univ. Carlos III de Madrid
Leganes, Spain
andres.barrado@uc3m.es

Joaquin Vaquero
M.A.C.I.M.T.E
Univ. Rey Juan Carlos
Mostoles, Spain
joaquin.vaquero@urjc.es

Yann E. Bouvier
M.A.C.I.M.T.E
Univ. Rey Juan Carlos
Mostoles, Spain
yann.bouvier@urjc.es

Carlos Pavon-Vargas
D.I.E.M
Univ. degli Studi di Salerno
Fisciano, Italy
cpavonvargas@unisa.it

Alejandro Stowhas
Electronics Department
Univ. Tecnica Federico Sta. Maria
Valparaiso, Chile
alejandro.stowhas@usml.cl

***Abstract*—Dual Active Bridge (DAB) converters have emerged as a leading solution for industrial applications that require high efficiency and bidirectional power transfer with isolation. The Triple-Phase-Shift (TPS) modulation scheme enables flexibility to enhance efficiency by choosing the operating point that minimizes power losses. This paper presents a novel, simplified methodology for reducing conduction losses in DAB converters using polynomial-based techniques. The operation of the DAB converter under TPS modulation is analyzed, and the corresponding modeling equations are derived. The proposed optimization method is described and validated through simulations in various design scenarios. The results demonstrate the existence of a set of three polynomials that effectively minimize the rms current based on the load conditions and the voltage ratio. Preliminary findings show that these polynomials will remain nearly constant across different converter designs, provided the output-to-input voltage ratio is the same.**

***Index Terms*—Dual-Active-Bridge, Triple-Phase-Shift, Current minimization, Polynomial.**

I. Introduction

Introduced in the early 90s, the Dual Active Bridge (DAB) converter, shown in Fig. 1, has become a well-known solution for applications requiring high efficiency, high power density, bidirectional power transfer, and galvanic isolation such as DC microgrids, Energy Storage Systems and Solid State Transformers [1]–[3].

Several modulation strategies have been developed to increase the DAB converter's performance possibilities. The Triple Phase Shift (TPS) modulation method unifies all previously proposed symmetrical phase-shifted approaches, and

The authors appreciate the financial support from Ministerio de Ciencia e Innovación under the project PID2023-152292OB-I00 and project TED2021-130613B-I00, the "UE - Ministerio de Hacienda y Función Publica - Fondos Europeos - Junta de Andalucía – Consejería de Universidad, Investigación e Innovación project 2024-31824 - 1828102303", ANID/FONDAP/1523A0006 SERC Chile, the European Union-NextGenerationEU/PRTR-C17.I1, the Community of Madrid, and MCIN / AEI / 10.13039/501100011033 through the research project GREENH2CM also de AEI /PID 2023-151697OA-100 through the research project PVCAD and by Univ. Rey Juan Carlos 2024-IMPULSO grant within its internal Research Promotion Program.

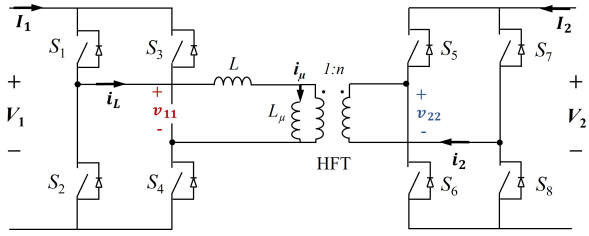


Fig. 1. Simplified DAB converter scheme.

considers three degrees of freedom to operate the DAB converter: internal phase-shift between the legs in the primary bridge (D_1), and internal phase-shift in the secondary bridge (D_2), and a phase shift between the two differential signals generated in the bridges (φ). Recent studies point-out that asymmetrical and hybrid-symmetrical modulation schemes widen the Zero Voltage Switching (ZVS) [4] at the cost of high complexity to the analysis and the practical implementation. Considering TPS as a good a compromise between flexibility and complexity, researchers have focused on optimizing DAB converter's performance from multiple perspectives: widening the soft-switching range, reducing backflow power, minimizing circulating power, and decreasing peak and effective (rms) current stresses [2], [5], [6]. The available optimization methods can be fundamentally categorized as model-driven or data-driven.

Generally, model-driven optimization methods aim to derive closed-form solutions to adequately calculate the three control variables of the TPS method (D_1, D_2 and φ). Proposals usually involve complex equations that vary with the load and voltages [3], [6]–[8]. The key advantage of model-driven optimizations is the adaptability to specific scenarios.

However substantial prior knowledge is required which becomes increasingly complex in multi-objective optimizations and may not always lead to a straightforward solution. This

complexity usually increases time and resources demand for control implementation, and may discourage adopting complex modulation schemes.

Unlike model-driven optimization, numerical methods do not always require a mathematical description or prior knowledge, making them appropriate for complex scenarios with strong non-linear behavior, such as power conversion systems [2], [9]–[11]. This advantage has promote their adoption in industrial applications. The most relevant data-driven optimization approaches include meta-heuristics and Deep Learning (DL) algorithms. Despite their potential, data-driven methods has notable challenges as their effectiveness is heavily dependent on the quality of the data collected and on the training process. Also, the lack of mathematical models can pose stability risks, making their generalization a key concern.

This work introduces a new optimization method to enhance the DAB converter efficiency using polynomials to obtain adequate TPS control parameters. The proposal combines model-driven and data-driven approaches' strengths as it feeds model-obtained data to an Exhaustive Search Algorithm (ESA) whose solutions are later automatically fitted into 3rd-grade polynomials. The validity of the method is confirmed with detailed numerical and time simulations. Results confirm the proposal as a competitive, simpler alternative given the high coherence with already published results.

The rest of the manuscript is organized as follows: Section II revises the DAB converter operation with the TPS modulation method and provides the model equations. Section III defines the losses models. In Section IV the optimization problem and methodology are described. The validation of the proposal is provided in Section V while Section VI draws some conclusions about the findings.

II. DAB Converter Operation and Modeling

In the DAB converter topology depicted in Fig. 1, labels S_i denote the MOSFETs, chosen as the switching power devices in this application. Labels V_1, I_1, V_2 and I_2 define the DC voltages and average currents of the full bridges 1 and 2, respectively. The High-Frequency Transformer (HFT) (with a turn-ratio of $n = N_2/N_1$) allows isolated power transfer, while the series inductor, L, conforms the power transfer. The magnetization inductance L_μ is included as it affects the soft-switching operation.

The TPS modulation method gives three degrees of freedom to operate the DAB converter: D_1, D_2 and φ. The parameters D_1 and D_2 are normalized over half the switching period leading to a range of $0 \leq D_x \leq 1$. Notice that D_1 ratio is represented in the pulse-width of the first bridge voltage waveform v_{11}, and similarly, D_2 in the pulse-width of the second bridge voltage waveform v_{22}. In contrast, φ is normalized to the entire switching period, T. The three control parameters shape the inductor voltage and, consequently, the current i_L profile, determining the the power transfer characteristics.

Each different i_L profile is called here Mode. Applying the TPS modulation method, seven Modes are found for each direction of the power transfer [12]. However, only four Modes

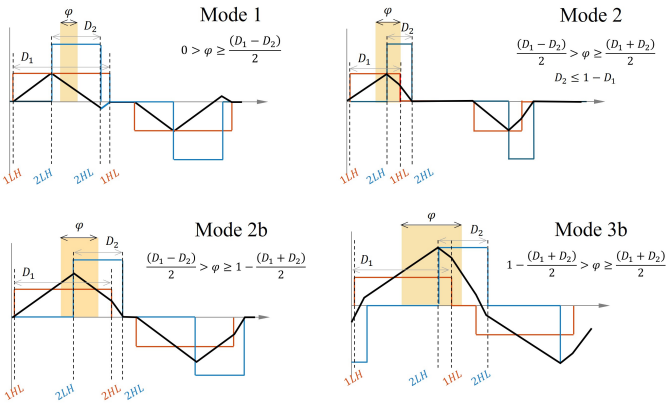


Fig. 2. Useful operating Modes of the DAB converter with TPS modulation.

are interesting for the DAB converter analysis, as they require lower rms current to deliver the same power than others [13]. Fig. 2 summarizes the interesting Modes for forward transmission and boost operation: Mode 1, Modes 2 and 2b, and Mode 3b. Each Mode presents different equations to determine the inductance current i_L at the switching instants ($1LH$, $1HL$, $2LH$ and $2HL$), the rms inductor current $i_{L,rms}$, the average input and output currents, I_1 and I_2, and the transferred power. Table I provides the main analytical equations. The switching instant expressions depending on the control parameters are:

$$\begin{aligned} 1LH &= (T/4)(1 - D_1) \\ 1HL &= (T/4)(1 + D_1) \\ 2LH &= (T/4)(2\varphi + 1 - D_2) \\ 2HL &= (T/4)(2\varphi + 1 + D_2) \end{aligned} \tag{1}$$

The analysis and the methodology described in the next sections are similar for boost/buck modes in forward/backward operations. Only the boost operation is discussed in this work, as it presents the worst case for the inductor design.

III. Power Loss Model

This section summarizes the loss models of the DAB converter and the assumptions made. The conduction losses P_{cond}, switching losses P_{sw}, and the core losses P_{core} are taken into account to calculate P_{tot} to evaluate the efficiency:

$$P_{tot} = P_{cond} + P_{sw} + P_{core} \tag{2}$$

A. Conduction Losses

Conduction losses comprise two terms: transistors' conduction loss $P_{cond,t}$, and magnetics' conduction loss $P_{cond,w}$.

The term $P_{cond,t}$ assumes that the conduction losses of the four transistors in each bridge are equal. Its calculation requires the value of the squared rms current in every Mode for the transistors involved $i_{rms,Si}$ and information about the on-resistance at the operation temperature of the MOSFETs in both bridges.

$$P_{cond,t} = 4\, i^2_{rms,S1} \cdot R_{DS,S1} + 4\, i^2_{rms,S5} \cdot R_{DS,S5} \tag{3}$$

TABLE I
ANALYTICAL EXPRESSIONS OF THE INDUCTOR AND MAGNETIZING CURRENTS CURRENTS AND TRANSFERRED POWER

	Inductor current	Magnetizing current	Power
Mode 1	$i_L(1LH) = \frac{T\,(D_2\,V_2 - D_1\,V_1\,n)}{4\,L\,n}$ $i_L(1HL) = -\frac{T\,(D_2\,V_2 - D_1\,V_1\,n)}{4\,L\,n}$ $i_L(2LH) = \frac{D_2\,T\,V_2}{4\,L\,n} - \frac{T\,V_1\,(D_2 - 2\,\varphi)}{4\,L}$ $i_L(2HL) = \frac{T\,V_1\,(D_2 + 2\,\varphi)}{4\,L} - \frac{D_2\,T\,V_2}{4\,L\,n}$	$i_\mu(1LH) = -\frac{D_2\,T\,V_2}{4\,L_\mu\,n}$ $i_\mu(1HL) = \frac{D_2\,T\,V_2}{4\,L_\mu\,n}$ $i_\mu(2LH) = -\frac{D_2\,T\,V_2}{4\,L_\mu\,n}$ $i_\mu(2HL) = \frac{D_2\,T\,V_2}{4\,L_\mu\,n}$	$\frac{D_2\,T\,V_1\,V_2\,\varphi}{2\,L\,n}$
Mode 2 & 2b	$i_L(1LH) = \frac{T\,(D_2\,V_2 - D_1\,V_1\,n)}{4\,L\,n}$ $i_L(1HL) = \frac{D_1\,T\,V_1}{4\,L} - \frac{T\,V_2\,(D_1 - 2\,\varphi)}{4\,L\,n}$ $i_L(2LH) = \frac{D_2\,T\,V_2}{4\,L\,n} - \frac{T\,V_1\,(D_2 - 2\,\varphi)}{4\,L}$ $i_L(2HL) = -\frac{T\,(D_2\,V_2 - D_1\,V_1\,n)}{4\,L\,n}$	$i_\mu(1LH) = -\frac{D_2\,T\,V_2}{4\,L_\mu\,n}$ $i_\mu(1HL) = \frac{T\,V_2\,(D_1 - 2\,\varphi)}{4\,L_\mu\,n}$ $i_\mu(2LH) = -\frac{D_2\,T\,V_2}{4\,L_\mu\,n}$ $i_\mu(2HL) = \frac{D_2\,T\,V_2}{4\,L_\mu\,n}$	$\frac{T\,V_1\,V_2\left(-{D_1}^2+2\,D_1\,D_2+4\,D_1\,\varphi-{D_2}^2+4\,D_2\,\varphi-4\,\varphi^2\right)}{16\,L\,n}$
Mode 3b	$i_L(1LH) = -\frac{D_1\,T\,V_1}{4\,L} - \frac{T\,V_2\,(D_1 + 2\,\varphi - 2)}{4\,L\,n}$ $i_L(1HL) = \frac{D_1\,T\,V_1}{4\,L} - \frac{T\,V_2\,(D_1 - 2\,\varphi)}{4\,L\,n}$ $i_L(2LH) = \frac{D_2\,T\,V_2}{4\,L\,n} - \frac{T\,V_1\,(D_2 - 2\,\varphi)}{4\,L}$ $i_L(2HL) = -\frac{T\,V_1\,(D_2 + 2\,\varphi - 2)}{4\,L} - \frac{D_2\,T\,V_2}{4\,L\,n}$	$i_\mu(1LH) = \frac{T\,V_2\,(D_1 + 2\,\varphi - 2)}{4\,L_\mu\,n}$ $i_\mu(1HL) = \frac{T\,V_2\,(D_1 - 2\,\varphi)}{4\,L_\mu\,n}$ $i_\mu(2LH) = -\frac{D_2\,T\,V_2}{4\,L_\mu\,n}$ $i_\mu(2HL) = \frac{D_2\,T\,V_2}{4\,L_\mu\,n}$	$-\frac{T\,V_1\,V_2\left({D_1}^2-2\,D_1+{D_2}^2-2\,D_2+4\,\varphi^2-4\,\varphi+2\right)}{8\,L\,n}$

Although the waveforms of each transistor are different, the rms current value is the same for all transistors within a full bridge. Rms currents are obtained by integrating the current of S_1 and S_5 for the Modes of interest. Equation (4) is an example of how $i_{rms,S1}$ current is calculated in Mode 1. Current $i_{rms,S5}$ has the same structure but integrates i_2.

$$\begin{aligned} i_{rms,S1\ Mode1} = \frac{1}{T}\Bigg(& \int_{1LH}^{2LH} (i_L(2LH))^2 dt \\ & + \int_{2LH}^{2HL} (i_L(2HL))^2 dt + \int_{2HL}^{1HL} (i_L(1HL))^2 dt \\ & + \int_{1HL}^{1LH+T/2} (-i_L(1LH))^2 dt \Bigg) \end{aligned} \tag{4}$$

The sum of the conduction loss of both the inductor and the HFT represents the term $P_{cond,w}$:

$$P_{cond,w} = P_{cond,L} + P_{cond,HFT} \tag{5}$$

being the conduction losses modeled as the multiplication of the rms current by the ESR (Equivalent Series Resistance) of the wire. In the case of the inductor L, the conduction loss is calculated as:

$$P_{cond,L} = i_{rms,L}^2 \cdot ESR_L \tag{6}$$

where the rms inductor current is calculated with (1) and Table I, depending on the Mode. Calculating the rms current involves partial integration and requires substituting the definition limits with the appropriate information given in (1) and Table I.

The conduction loss model for the HFT includes both the primary and secondary windings:

$$P_{cond,HFT} = i_{rms,L}^2 \cdot ESR_{N1} + i_{rms,2}^2 \cdot ESR_{N2} \tag{7}$$

$$i_{rms,2}^2 = \frac{1}{n}\int_0^T \Big(i_L\ (t) - i_\mu\ (t)\Big)^2 dt \tag{8}$$

The rms current in the secondary winding is calculated considering the magnetization current i_μ and the turn ratio n.

The equivalent series resistance, ESR, of the wires is calculated with the number of turns N, the resistivity, ρ, the total section of the wire, A_w, and the MLT (Mean Length per Turn) data, usually provided by the manufacturer. As ρ varies with temperature, application's worst case is used.

$$ESR = (\rho \cdot N \cdot MLT)/A_w \tag{9}$$

B. Switching Losses

The switching losses of the DAB converter are estimated with (10) applied to each transistor. On it R_g is the total gate resistance, Q_{gs} and Q_{gd} are the gate-to-source and gate-to-drain charges, and $V_{plateau}$ is the Miller voltage.

$$\begin{aligned} P_{sw} &= P_{sw,\ ON} + P_{sw,\ OFF} \\ P_{sw,\ ON} &= 0.5\,(t_{on} \cdot V_{ds} \cdot i_{on}) \cdot f \\ t_{on} &= R_g\,(Q_{gs} + Q_{gd})/(V_{gs} - V_{plateau}) \\ P_{sw,\ OFF} &= 0.5\,(t_{off} \cdot V_{ds} \cdot i_{off}) \cdot f \\ t_{off} &= R_g\,(Q_{gs} + Q_{gd})/V_{plateau} \end{aligned} \tag{10}$$

The values instant currents, i_{on} and i_{off} are equal $-i_{on}$ due to waveform symmetry and are obtained using the information in Table I and in Fig. 2.

The analysis in this paper considers that a negative value in (10) implies soft-switching in the evaluated transistor and is taken as a loss of 0 Watts. The potential masking of incomplete soft-switching is acknowledged, but assumed to help the intended practical simplified proposal.

C. Core Loss

Core losses are determined by the sum of the core loss in the inductor $P_{core,L}$ and in the transformer $P_{core,HFT}$.

The Modified Steinmetz Equation (MSE) approach [14] is chosen to model the core loss of the magnetic components, as the voltage waveform applied to the magnetics in the DAB converter is not sinusoidal:

$$\begin{aligned} P_{core} &= Vol \cdot f \left(C_m \cdot f_{eq}^{\alpha-1} \cdot \left(\frac{\Delta B}{2} \right)^{\beta} \right) \\ f_{eq} &= \frac{2}{\Delta B^2 \pi^2 \cdot N^2 A_e^2} \int_0^T \left(\frac{dv_x(t)}{dt} \right)^2 dt \\ B(t) &= \frac{1}{N A_e} \int v_x(t)\, dt \\ \Delta B &= \max(B(t)) - \min(B(t)) \end{aligned} \tag{11}$$

where Vol and A_e are the effective volume and area of the core respectively, and N is the number of turns (of the primary in the case of the HFT) of the component evaluated. Manufacturers usually provide Steinmetz coefficients C_m, β, and α. Voltage v_x is that applied to the evaluated component winding (inductor's or HFT's primary).

IV. Proposed minimization strategy

A. Formulation of the minimization problem

Maximizing the efficiency of the DAB converter implies the minimization of the power losses (2). Conduction losses are usually a main concern of the DAB operation, so minimizaion of the rms inductor current is a research priority. Deeply related to the current peak, rms current reduction also minimizes core loss. [5], [7].

This work aims to improve the operation of the DAB by defining the minimization problem specified in (12), where $m = V_2/(nV_1)$:

$$\begin{cases} Obj.1 = \min(i_{rms,L}, m) \\ Obj.2 = \min(P_{tot}(i_{rms,L}), m) \\ Constr. = P \end{cases} \tag{12}$$

The first objective, *Obj. 1*, is to minimize the rms inductor current for a given power P specification *Constr. 1*. In the case that several values of the TPS control parameters obtain the same rms inductor current, those with the lowest total loss calculated with (2) will be selected according to *Obj. 2*.

A new methodology is proposed to enhance the DAB converter operation by choosing the TPS control parameters fulfilling (12) with a closed-form equation, defining their evolution over the power range for a given m. Fig. 3 shows the flowchart of the proposed method. First, the reduced-order model of the DAB converter with the TPS modulation is combined with power loss models to construct a comprehensive map of the operating points. Then, using an Exhaustive Search Algorithm (ESA), the operating points for problem minimization across the power range are identified offline, by their control parameters (φ, D_1, and D_2). Later, a polynomial expression for each TPS control parameter is derived using an automatic linearization algorithm.

B. Data generation and searching stage

Offline, for a designed DAB converter (transistors, inductor, and HFT are known) and a given specification (V_1, V_2, and f), all data of interest to evaluate the DAB performance over the entire range of variation of the TPS parameters are calculated, for the operating Modes of the converter shown in Fig. 2. Later, an ESA is performed looking for the operation points that minimize (12) over the power range. The points generated conform the $T1$ trajectory of the control parameters.

Considering the design of the DAB_1 summarized in Table II for m = 2 the results found by the ESA are shown in Fig. 4 depicted in gray. At this point of the process, the results are not linear and present abrupt variations depending on the precision of the calculus and the sweep accuracy while generating the searching map.

C. Automatic linearization of the TPS control parameters

The TPS control parameters found in the previous step are processed using an automatic linear regression algorithm to smooth the results. Linear regression method is chosen due to its simplicity and widespread use as a suitable approach for modeling the data. The algorithm progressively increases the degree of the polynomial until it meets two criteria: an R-squared value greater than 90%, and an increase in the degree that does not improve the fit by more than 1%. The dimensionless, independent variable in the fitting is named here K_{vp}, defined in (13) and considers constant V_1:

$$K_{vp} = \frac{P}{P_{nom}} \frac{m_{nom}}{m} \tag{13}$$

Fig. 4 shows the obtained linearized solution of the TPS control parameters.

V. Validation

This section provides validation of the proposed methodology by testing it in a variety of contexts to show its potential.

First, the adaptability of the method to different specifications is tested with detailed numerical simulations. Table II summarizes the specifications for three different DAB converter designs chosen to emphasize the validity of the proposed method and the consistency of the results.

The design DAB_1 is sized to have balanced the switching and the conduction losses, while the other two designs (DAB_2 and DAB_3) push further the conduction losses and the switching loss respectively. The inductance L is designed to ensure that the maximum allowable power transfer is the maximum



Fig. 3. Flow diagram of the proposed method.

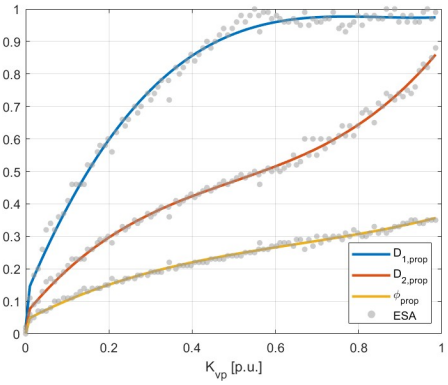


Fig. 4. Solutions of the TPS control parameters over the power range.

TABLE II
SPECIFICATIONS OF THE DAB CONVERTER DESIGNS

Param.	DAB_1	DAB_2	DAB_3
V_1	$200\,V$	$200\,V$	$200\,V$
V_2	$[280-400]\,V$	$400\,V$	$400\,V$
f	$50\,kHz$	$50\,kHz$	$500\,kHz$
P_{max}	$550\,W$	$1100\,kW$	$550\,W$
L	$364\,\mu H$ $P42/29$ $3C95$ $N=56$ $1400x0.04\,(x1)$	$181\,\mu H$ $P42/29$ $3C95$ $N=56$ $1400x0.04\,(x1)$	$36.4\,\mu H$ $ETD34/17/11$ $3F36$ $N=48$ $1400x0.04\,(x1)$
HFT	$36\,mH$ $E65/32/27$ $3C95$ $n=64:64$ $1400x0.04\,(x1)$	$18\,mH$ $E65/32/27$ $3C95$ $n=64:64$ $1400x0.04\,(x1)$	$3.6\,mH$ $PQ35/35$ $3F36$ $n=26:26$ $1400x0.04\,(x1)$
$Transistor$	IMW65R107M1H		

power P_{max} when the TPS control parameters are at their maximum values (D_1 = D_2 = 1, and φ = 0.5) which is a common practice for a widened ZVS region [15].

Fig. 5 shows the results of the three different DAB designs, where the curves corresponding to the TPS control parameters obtained by the optimization problem are practically superimposed. As the power transfer depends on V_1, V_2, T and L as shown in Table I, the expected rms current minimization will remain the same if the relationship between these parameters keeps the same. Therefore, once all the specification values are settled, the resultant polynomials will only vary according to m for a normalized power range.

For the designs studied, the solutions of the proposed method produce a non-obvious conclusion: a 3rd-order polynomial gets the expected rms current minimization fulfilling the confidence criteria. The existence of polynomials providing the required minimization implies an improvement over previous data-driven and model-driven works regarding control simplicity, robustness, and computing consumption.

The proposed method is compared with [8] and [9], which are acknowledged as good examples of model-driven and data-driven methodologies, respectively. Fig. 6 shows the D_1 and D_2 trajectories published in said references, with the proposed solution superimposed. As shown, the proposal's trajectories are close to the solution in [8] along most of the power range, as the data come in both cases from analytical modeling. In contrast to [9], the proposal does not use experimental data during the optimization process. As a result, the outcomes differ, although the trajectories exhibit similar trends. Finally, Fig. 7 shows the time simulation of the inductor current for $K_{vp} = 0.25$ (marked with a dotted line in Fig. 6), comparing the proposal with the referenced approaches. The results validate the proposed method's effectiveness in reducing power losses in DAB converters, showing strong consistency with the previously published approaches.

VI. CONCLUSION

A novel optimization method is proposed, combining model-driven and data-driven optimization approaches' strengths, to achieve a simplified, linear solution for computing TPS control parameters to minimize rms current in the series inductor of the DAB converter. The proposed method uses polynomial fitting of the TPS parameters trajectories previously obtained within analytical data points using ESA. The obtained polynomials enable the required operation across the power range and ensure smooth transitions between Modes with minor error compared to purely analytical results.

Key insights from the designs used for validation highlight that a 3rd-order polynomial is sufficient to meet confidence requirements. Once the DAB design is defined, preliminary results show the polynomial order and coefficients will remain nearly constant across different converter designs, provided the m ratio stays the same.

The findings imply a significant improvement over previous works since the simplicity achieved offers enhanced control robustness and low computational burden. Also, the proposal reduces the time to achieve an optimized solution and simplifies implementation, making it more accessible for practical applications.

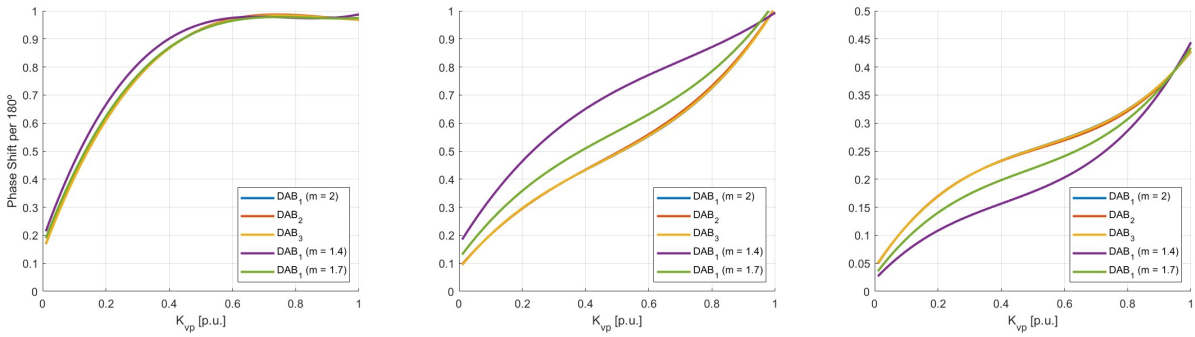


Fig. 5. TPS control parameters trajectory obtained with the proposed method for various DAB designs. D_1 (left), D_2 (center) and φ (right).

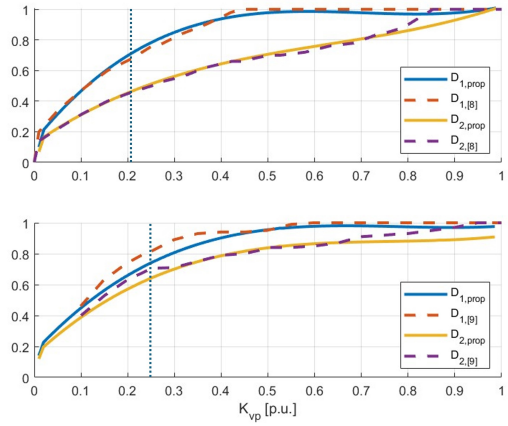


Fig. 6. Comparison of D_1, and D_2 trajectories fulfilling the minimization goal: with [8] (top); with [9] (bottom).

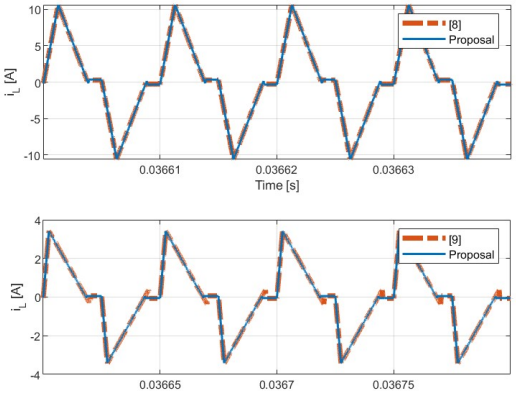


Fig. 7. Time simulation of the proposal compared to the results in [8] (top), and [9] (bottom) for $K_{vp} = 0.25$.

REFERENCES

[1] Q. Xu, N. Vafamand, L. Chen, T. Dragicevic, L. Xie, and F. Blaabjerg, "Review on advanced control technologies for bidirectional dc/dc converters in dc microgrids," *IEEE Journal of Emerging and Selected Topics in Power Electronics*, vol. 9, pp. 1205–1221, 4 2021.

[2] L. Zhou, Y. Gao, H. Ma, and P. T. Krein, "Wide-load range multiobjective efficiency optimization produces closed-form control solutions for dual active bridge converter," *IEEE Transactions on Power Electronics*, vol. 36, pp. 8612–8616, 8 2021.

[3] Z. Guo, "Modulation scheme of dual active bridge converter for seamless transitions in multiworking modes compromising zvs and conduction loss," *IEEE Transactions on Industrial Electronics*, vol. 67, pp. 7399–7409, 9 2020.

[4] M. Mahdavifard and S. A. Khajehoddin, "Closed-form continuous asymmetrical hybrid modulation, ensuring wide zvs range and seamless transients for dab converters," *IEEE Transactions on Power Electronics*, vol. 39, pp. 5776–5792, 5 2024.

[5] N. Noroozi, A. Poorfakhraei, O. Zayed, A. Elezab, N. Keshmiri, M. Narimani, and A. Emadi, "Rms current minimization in a sic-based dual active bridge converter using triple-phase-shift modulation," *IEEE Transactions on Industrial Electronics*, vol. 70, pp. 7173–7182, 7 2023.

[6] L. Gong, X. Jin, J. Xu, Z. Deng, H. Li, T. B. Soeiro, and Y. Wang, "A dynamic zvs-guaranteed and seamless-mode-transition modulation scheme for the dab converter that maximizes the zvs range and lowers the inductor rms current," *IEEE Transactions on Power Electronics*, vol. 37, pp. 13 119–13 134, 11 2022.

[7] A. Tong, L. Hang, G. Li, X. Jiang, and S. Gao, "Modeling and analysis of a dual-active-bridge-isolated bidirectional dc/dc converter to minimize rms current with whole operating range," *IEEE Transactions on Power Electronics*, vol. 33, pp. 5302–5316, 6 2018.

[8] F. Krismer and J. W. Kolar, "Closed form solution for minimum conduction loss modulation of dab converters," *IEEE Transactions on Power Electronics*, vol. 27, pp. 174–188, 2012.

[9] X. Li, X. Zhang, F. Lin, C. Sun, and K. Mao, "Artificial-intelligence-based triple phase shift modulation for dual active bridge converter with minimized current stress," *IEEE Journal of Emerging and Selected Topics in Power Electronics*, vol. 11, pp. 4430–4441, 8 2023.

[10] S. Izadi, M. Izadi, K. Jabari, and B. Zaker, "Enhancing efficiency in bidirectional dc-dc converters through pso-based optimization." Institute of Electrical and Electronics Engineers Inc., 2024.

[11] A. A. Ibrahim, A. Zilio, T. Younis, D. Biadene, T. Caldognetto, and P. Mattavelli, "Optimal modulation of triple active bridge converters by an artificial-neural- network approach," *IEEE Transactions on Industrial Electronics*, vol. 71, pp. 2590–2600, 3 2024.

[12] C. Calderon, A. Barrado, A. Rodriguez-Lorente, P. Alou, A. Lazaro, C. Fernandez, and P. Zumel, "General analysis of switching modes in a dual active bridge with triple phase shift modulation," *Energies*, 2018.

[13] C. Calderon, A. Barrado, A. Rodriguez, A. Lazaro, M. Sanz, and E. Olías, "Dual active bridge with triple phase shift, soft switching and minimum rms current for the whole operating range," in *IECON 2017 - 43rd Annual Conference of the IEEE Industrial Electronics Society*, 2017, pp. 4671–4676.

[14] J. Reinert, A. Brockmeyer, and R. De Doncker, "Calculation of losses in ferro- and ferrimagnetic materials based on the modified steinmetz equation," *IEEE Transactions on Industry Applications*, vol. 37, no. 4, pp. 1055–1061, 2001.

[15] A. R. Rodriguez Alonso, J. Sebastian, D. G. Lamar, M. M. Hernando, and A. Vazquez, "An overall study of a dual active bridge for bidirectional dc/dc conversion," in *2010 IEEE Energy Conversion Congress and Exposition*, 2010, pp. 1129–1135.